Hindawi Publishing Corporation
International Journal of Photoenergy
Volume 2013, Article ID 280253, 8 pages
http://dx.doi.org/10.1155/2013/280253

Research Article

Dye-Sensitized Solar Cells with Anatase TiO_2 Nanorods Prepared by Hydrothermal Method

Ming-Jer Jeng,[1] Yi-Lun Wung,[1] Liann-Be Chang,[1] and Lee Chow[2]

[1] *Department of Electronic Engineering and Green Technology Research Center, Chang-Gung University, Taoyuan 333, Taiwan*
[2] *Department of Physics, University of Central Florida, Orlando, FL 32816, USA*

Correspondence should be addressed to Ming-Jer Jeng; mjjeng@mail.cgu.edu.tw

Received 29 June 2013; Revised 20 August 2013; Accepted 6 September 2013

Academic Editor: Stefano Caramori

The hydrothermal method provides an effective reaction environment for the synthesis of nanocrystalline materials with high purity and well-controlled crystallinity. In this work, we started with various sizes of commercial TiO_2 powders and used the hydrothermal method to prepare TiO_2 thin films. We found that the synthesized TiO_2 nanorods were thin and long when smaller TiO_2 particles were used, while larger TiO_2 particles produced thicker and shorter nanorods. We also found that TiO_2 films prepared by TiO_2 nanorods exhibited larger surface roughness than those prepared by the commercial TiO_2 particles. It was found that a pure anatase phase of TiO_2 nanorods can be obtained from the hydrothermal method. The dye-sensitized solar cells fabricated with TiO_2 nanorods exhibited a higher solar efficiency than those fabricated with commercial TiO_2 nanoparticles directly. Further, triple-layer structures of TiO_2 thin films with different particle sizes were investigated to improve the solar efficiency.

1. Introduction

Dye-sensitized solar cells (DSSCs) have attracted much attention as possible candidates for low cost, high stability, and high efficient solar cells [1, 2]. There are many innovations in this emerging technology such as new dyes which are absorbed at a wider range of wavelengths and the introduction of nanostructure titanium oxides (TiO_2) to increase the surface area [3–5]. The DSSCs with the nanostructure titanium oxide/Porphyrins dye thin films on transparent conducting oxide- (TCO-) coated glass can achieve a solar efficiency as high as 13% [6]. The major improvements of the research are made not only by introducing highly absorbing dyes as light harvesters, but also by using the nanostructure layer to improve the absorption and collection efficiency. In principle, fast electron transport and slow recombination will be needed to obtain a high solar conversion efficiency. For conventional DSSC, the mesoporous film consisted of nanocrystalline TiO_2 particles, enjoying the advantages of a large surface for greater dye adsorption and facilitating electrolyte diffusion within their pores [7–12]. The hydrothermal method provides an effective reaction environment for the synthesis of nanocrystalline TiO_2 with high purity and well-controlled crystallinity [13–15]. Therefore, we use the hydrothermal method to prepare TiO_2 thin films in this work. The Taguchi method [16–20] is used to find the optimal parameters for the formation of high-quality TiO_2 films. The Taguchi method [16] is a process optimization technique that investigates how multiparameters affect the performance of a process. It can minimize the variation in a process through robust design of experiments. The Taguchi method uses orthogonal arrays [17] to organize the parameters affecting the process and the levels at which they should be varied. It allows for the determination of factors mostly affecting a process performance characteristic with a minimum amount of experimentation. Generally, it employs a generic signal-to-noise (S/N) ratio to quantify the variation. These S/N ratios are used as measures of the effect of noise factors on performance characteristics. There are several S/N ratio types of characteristics: larger is better, nominal is best, smaller is better, and so forth [16, 18].

In addition, it is known that the strong back-scattering light due to the large particles near the conducting glass results in a light loss. To reduce light loss due to this strong back-scattering light, multiple-layer structure of TiO_2 with

Table 1: Level of process parameters.

Symbol	Factor level	1	2	3
A	NaOH concentration (M)	10	8	12
B	TiO_2 particle size (nm)	14	21	100
C	Autoclave temperature (°C)	180	200	230
D	Annealing temperature (°C)	450	500	550

different particle sizes has been proposed in the past [21–27]. Here triple TiO_2 layer structure with small particle sizes is at the bottom, medium sizes in the middle, and large particle sizes on top which are also investigated to improve the solar performance of DSSCs.

2. Experiments

The 2 cm × 1.5 cm fluorine-doped SnO_2- (FTO-) coated glass electrodes (sheet resistance 8 Ω/□) were cleaned by acetone, isopropanol, and deionized water sequentially. In the hydrothermal procedure, 3 g TiO_2 powders were placed into a Teflon lined autoclave of 100 mL capacity. The autoclave was filled with 8 M, 10 M, or 12 M NaOH aqueous solution and sealed into a stainless steel tank and maintained at 180°C for 24 hrs. It was cooled down naturally to room temperature. The obtained sodium titanate was put into 200 mL of 1 N HCl aqueous solution at pH = 2 and stirred for 24 h. This HCl treatment was repeated many times in order to exchange Na^+ ions completely by H^+ ions leading to the formation of hydrogen titanate nanorods. Then these hydrogen titanate nanorods were washed with distilled water until the pH reached 7 and filtered to obtain the precipitated hydrogen titanate nanorods. These nanorods were dehydrated and recrystallized into the anatase TiO_2 nanorods. Table 1 shows the four factors and three levels used in our experiment according to the Taguchi method [16–20]. If three levels were assigned to each of these factors, then conventional method would require 3^4 or 81 experiments to find the optimal condition. Using the Taguchi method, we can reduce the number of experiments to nine. The orthogonal array of L9 type [17] is used and shown in Table 2. This design requires nine experiments with four parameters at three levels of each. The interactions of these four parameters were neglected. TiO_2 solutions are prepared by mixing 3 g of TiO_2 powders, 1 mL of titanium tetraisopropoxide (TTIP), 0.5 g of Polyethylene glycol (PEG), and 0.5 mL of triton X-100 in 50 mL of isopropanol (IPA). The mixture was then grinded and stirred by zirconia ball for 8 hours. It is known that the addition of TTIP in the solution can reduce the surface crack and the PEG can make a porous thin film after annealing. The TiO_2 thin films were formed by spin-coating TiO_2 solutions on FTO-coated glass and annealed at 500°C for one hour. The coated TiO_2 photo-electrodes were then immersed for 24 hrs in a hydrous ethanol solution containing 3×10^{-4} M N719 dye. The liquid electrolyte consisted of 1 M lithium Iodide (LiI), 0.1 M Iodine (I_2), 0.5 M 4-tert-butyl pyridine (TBP), and 0.6 M 1,2-Dimethyl-3-propylimidazolium iodide (DMPII) in acetonitrile. The cathode electrode was made of

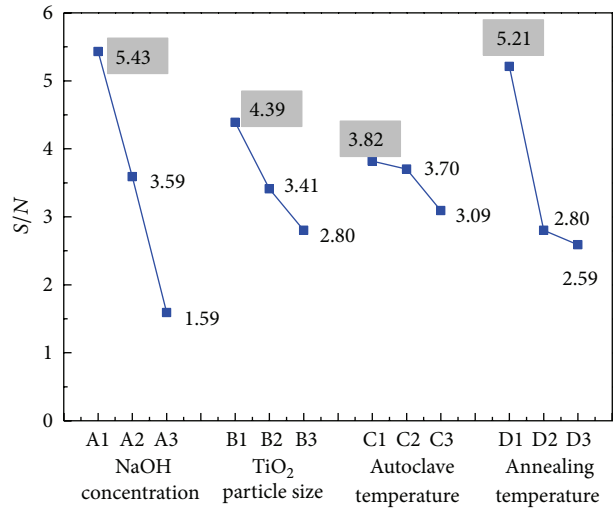

Figure 1: The factor effects on the S/N ratio.

FTO-coated glass, which was further coated with H_2PtCl_6 precursor and annealed at 450°C for 30 min. The cell was fabricated by applying a surlyn spacer, which is a hot-melting film with a thickness of 60 μm, between two electrodes. Two FTO-coated glasses were made with the surlyn heated at 100°C. The electrolyte was injected into the space between the electrodes by capillary action. Finally, these two FTO-coated glasses were sealed completely. The active area of cells is 1 cm^2. The photocurrent-voltage (I-V) characteristic curves were measured using Keithley 2420 under AM1.5G illumination.

3. Results and Discussions

Nine different hydrothermal experiments were performed using the design parameter combinations shown in Table 2. Three specimens were fabricated for each of the parameter combinations. The factor effects on the solar efficiency and S/N ratio for each experiment are listed in Table 3. The higher solar efficiency is the indication of better performance. Therefore, the larger-is-better criterion was selected for the solar efficiency to obtain the optimal solar performance. The following S/N ratios for the larger-is-better case can be calculated [16, 18]:

$$\left(\frac{S}{N}\right)_{\mathrm{LB}} = -10 \log \frac{\sum_{i=1}^{n} 1/(y_i)^2}{n}, \quad (1)$$

where $(S/N)_{\mathrm{LB}}$ stands for the larger-is-better signal-to-noise ratio, y_i is the individually measured solar efficiency, and n is the number of solar cell samples measured. Figure 1 shows the factor effects on the S/N ratio. The larger slope means that the factor has a stronger effect on solar efficiency. It indicates that NaOH concentration (factor A) has a stronger effect on solar efficiency. The annealing temperature (factor D) is the next most significant factor. The objective is to maximize the S/N ratio. This implies that one can obtain high solar efficiency by using the factor with higher S/N ratio. It is clear from Figure 1 that the highest S/N ratio values in each factor are

Table 2: Taguchi L9 orthogonal array.

Order	Factor			
	A NaOH concentration (M)	B TiO_2 particle size (nm)	C Autoclave temperature (°C)	D Annealing temperature (°C)
1	10 M	14 nm	180°C	450°C
2	10 M	21 nm	200°C	500°C
3	10 M	100 nm	230°C	550°C
4	8 M	14 nm	200°C	550°C
5	8 M	21 nm	230°C	450°C
6	8 M	100 nm	180°C	500°C
7	12 M	14 nm	230°C	500°C
8	12 M	21 nm	180°C	550°C
9	12 M	100 nm	200°C	450°C

Table 3: The factor effects on the solar efficiency and S/N ratio.

Factor				Efficiency (%)	S/N ratio
A NaOH concentration (M)	B TiO_2 particle size (nm)	C Autoclave temperature (°C)	D Annealing temperature (°C)		
1	1	1	1	2.31	7.27
1	2	2	2	1.80	5.11
1	3	3	3	1.57	3.92
2	1	2	3	1.27	2.08
2	2	3	1	2.06	6.28
2	3	1	2	1.32	2.41
3	1	3	2	1.11	0.91
3	2	1	3	1.23	1.80
3	3	2	1	1.27	2.08

5.43, 4.39, 3.82, and 5.21, which correspond to the factor A1, B2, C1, and D1, respectively. Therefore, the best parameters of hydrothermal methods are (A1) NaOH concentration of 10 M, (B2) commercial TiO_2 particle size of 21 nm, (C1) the temperature of 180°C, and (D1) the annealing temperature of 450°C. Thus, these best parameters were used to prepare our TiO_2 nanorods.

Figures 2(a) and 2(b) show the surface morphology of TiO_2 films prepared by commercial TiO_2 particles and TiO_2 nanorods which we prepared using hydrothermal methods, respectively. Clearly, a particle-like surface in the film is prepared using commercial particles versus a nanorod-shape surface in the film prepared by our TiO_2 nanorods. From atomic force microscopy (AFM) measurement, it is observed that the mean roughness (~63 nm) of the TiO_2 thin films prepared by the TiO_2 nanorods is larger than that (~41.5 nm) prepared by the commercial TiO_2 particles. The large surface roughness in TiO_2 nanorods is beneficial for dye adsorption. In addition, a very pure anatase structure of TiO_2 nanorods is obtained by the hydrothermal method, as shown in Figure 3. There are no characteristic peaks of other impurity phases such as sodium titanium oxide or rutile TiO_2, except pure anatase TiO_2 nanorods. This pure anatase structure of TiO_2 is extremely important to achieve high performance for electrons transport and dye adsorption in TiO_2-based dye-sensitized solar cells [28, 29]. Figure 4 compares the I-V characteristics of dye-sensitized solar cell prepared with hydrothermally grown TiO_2 nanorods and the DSSC prepared with commercial TiO_2 particles. The dye-sensitized solar cells prepared with the hydrothermally grown TiO_2 nanorods clearly exhibit higher solar efficiency than that prepared with the commercial TiO_2 particles. This is due to the fact that TiO_2 nanorods have large surface area and pure anatase structure, which can absorb more dye and therefore better photoresponse.

It is also noted that the size of TiO_2 nanorods synthesized by hydrothermal method depends on the initial TiO_2 particle size. The nanorods are thin and long when small-size TiO_2 particles (size ~14 nm) are used; however the nanorods become thick and short when large-size TiO_2 particles, are used (size, ~100 nm), as shown in Figures 5(a) and 5(b). One can control the shape of TiO_2 nanorods by suitably choosing the initial TiO_2 particle sizes used in the hydrothermal process. Next we will examine the effect of TiO_2 thin film thickness on the solar efficiency of the fabricated DSSCs. In Figure 6, the cross-section scanning electron microscopy (SEM) images of different thickness of TiO_2 thin films are shown. We can see that a nanorod-like morphology is observed when 21 nm TiO_2 powder is used in the hydrothermal reaction. The optical absorption and

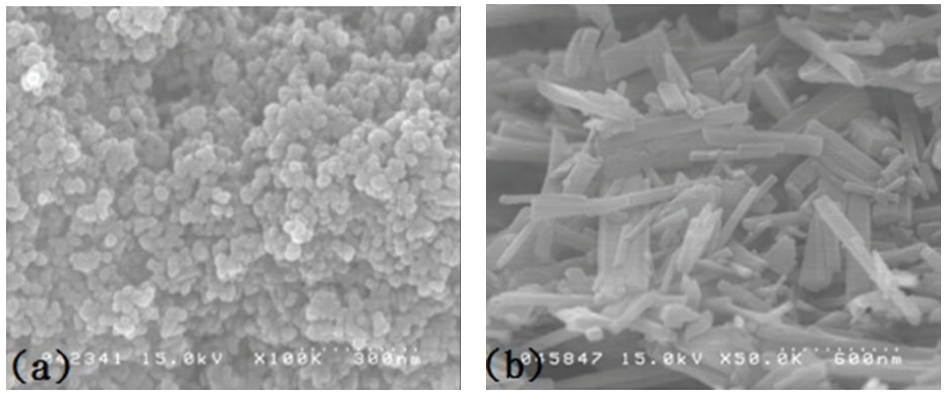

(a) (b)

Figure 2: Surface morphology of TiO_2 thin films prepared by (a) commercial particles and (b) hydrothermal method.

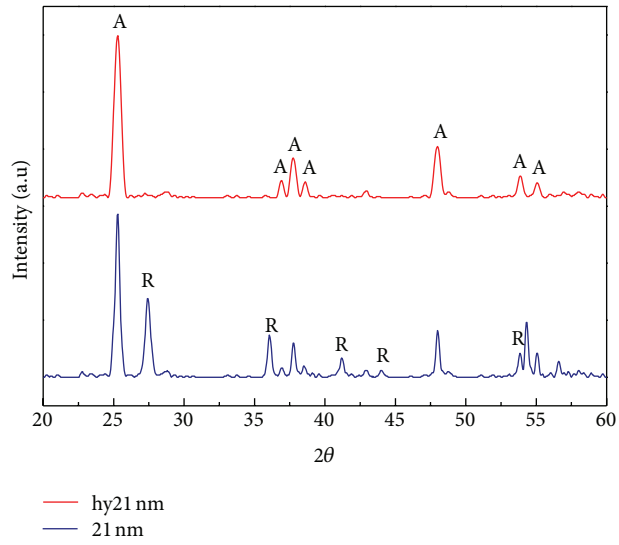

Figure 3: XRD spectra of TiO_2 thin films prepared by hydrothermal method (red color) and commercial particle (blue color).

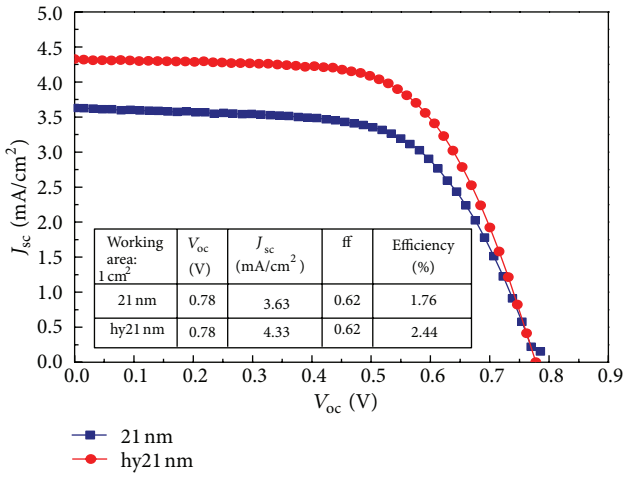

Figure 4: The *I-V* curve of dye-sensitized solar cells with the TiO_2 prepared by hydrothermal method and commercial particle.

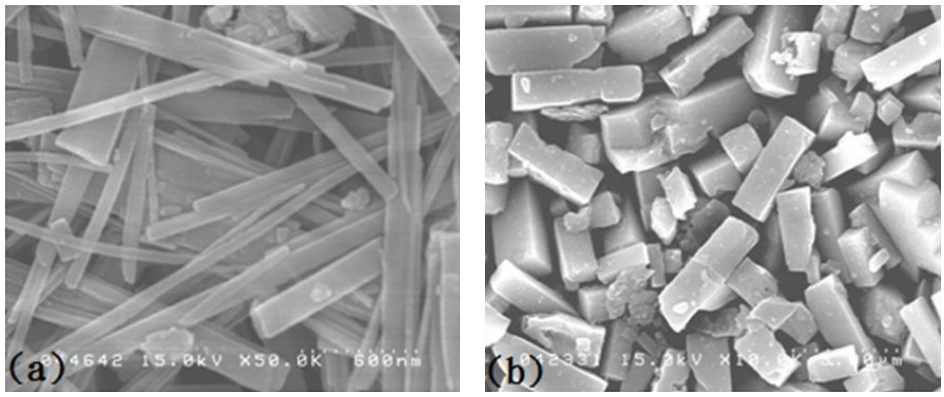

(a) (b)

Figure 5: Nanorod size dependence on the using of the particle size of (a) 14 nm and (b) 100 nm.

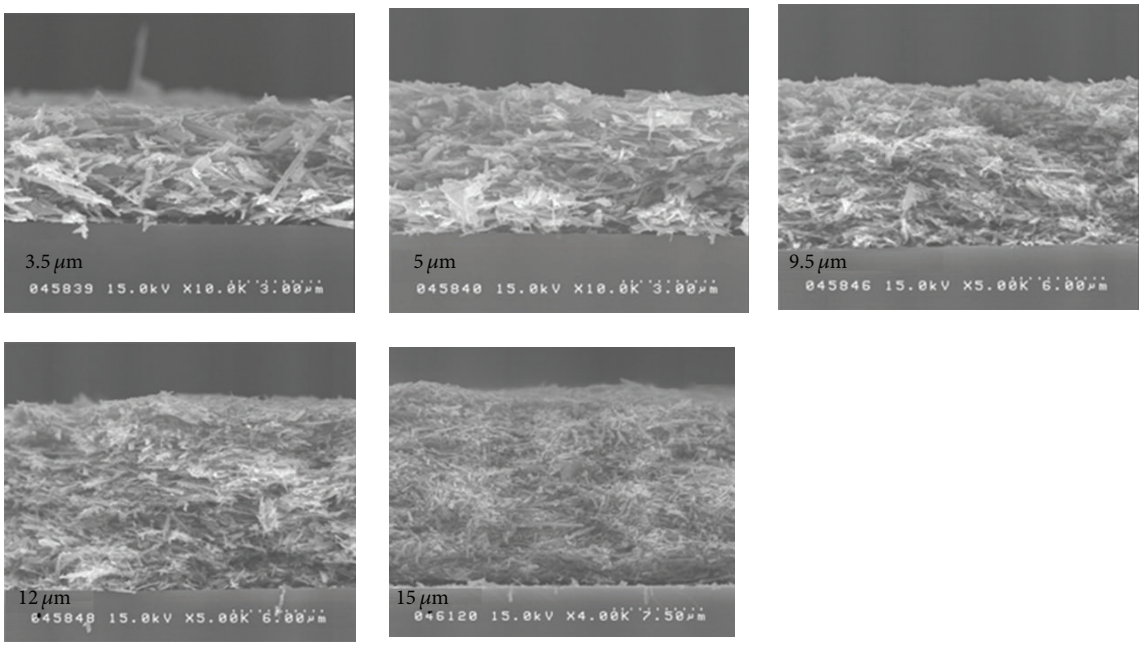

Figure 6: The cross-section scanning electron microscopy (SEM) images of TiO_2 thin films with different thicknesses.

I-V characteristic curve of dye-sensitized solar cells with different TiO_2 thicknesses are shown in Figures 7(a) and 7(b), respectively. The optical absorption initially increases with increasing TiO_2 thickness and reaches a maximum at 12 μm. For further increase in the TiO_2 film thickness, the light absorption begins to drop. The same behavior is observed in the photocurrent, as shown in Figure 7(b). The solar performance parameters of DSSCs with different TiO_2 thicknesses are listed in Table 4. The efficiencies of DSSCs with the TiO_2 thicknesses of 3.5, 5, 9.5, 12, and 15 μm are 2.12, 2.44, 2.63, 2.85, and 2.67%, respectively. The DSSC with the TiO_2 thicknesses of 12 μm exhibits the highest efficiency. It is known that dye in the film will build up with increasing TiO_2 thickness and hence increase the photocurrent. However, thicker TiO_2 layers will result in a decrease in the transmittance of light through these TiO_2 layers and thus reduce the incident light absorbed by the dyes. In addition, the charge recombination between electrons from the excited dye to the conduction band of TiO_2 and the I^{3-} ions in the electrolyte will become more difficult in thicker TiO_2 layers. Thus, there exists an optimal TiO_2 thickness to achieve higher solar efficiency for each particle size. In this work, the optimal TiO_2 thickness is 12 μm for particle size of 21 nm used in the hydrothermal reaction.

It is known that large-size TiO_2 particles have the advantage of strong light scattering ability, while small size TiO_2 particles have the advantages of large contact area and low contact resistance [18–24]. In order to take the advantages of both the strong light scattering and the large contact area/low contact resistance, we constructed a triple-layer TiO_2 DSSC

Table 4: Solar performance parameters of DSSCs with different TiO_2 thicknesses.

Working area: 1 cm^2	V_{oc} (V)	J_{sc} (mA/cm^2)	Fill factor	Efficiency (%)
3.5 um	0.79	3.63	0.62	2.12
5 um	0.76	4.73	0.62	2.44
9.5 um	0.77	5.25	0.64	2.63
12 um	0.76	5.89	0.63	2.85
15 um	0.76	5.58	0.62	2.67

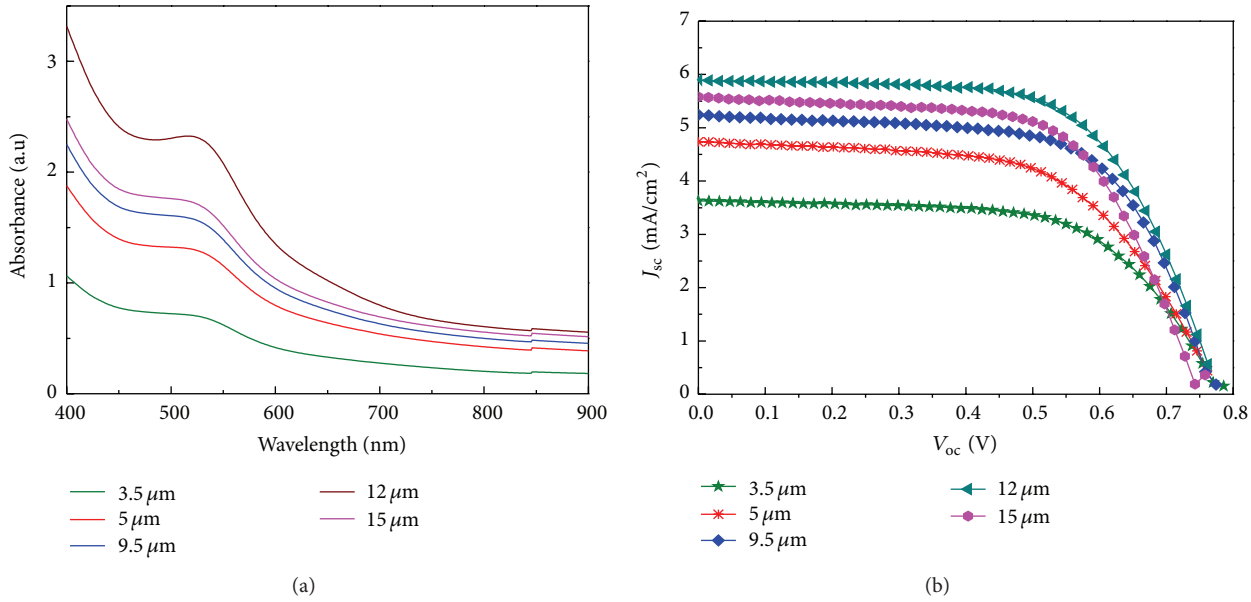

Figure 7: (a) Light absorption and (b) *I-V* curve of dye-sensitized solar cells with different TiO_2 thicknesses.

Table 5: Solar performance parameters of DSSCs with different particle sizes on the top in triple TiO_2 layers.

Particle size (nm)	V_{oc} (V)	J_{sc} (mA/cm^2)	Fill factor	Efficiency (%)
50/hy21/9/FTO	0.67	8.85	0.61	3.62
100/hy21/9/FTO	0.75	12.02	0.62	5.68
200/hy21/9/FTO	0.76	14.32	0.61	6.54

with varying TiO_2 particle size. The structure of the triple-layer TiO_2 DSSC is as follows: (1) a TiO_2 thin film prepared with 9 nm TiO_2 particles is on the bottom layer; (2) a TiO_2 film prepared with hydrothermally grown TiO_2 nanorods is placed on the middle layer; (3) on the top, TiO_2 films are prepared with three different sizes of 50 nm, 100 nm, and 200 nm TiO_2 nanorods used for comparison. Figure 8(a) shows the cross-sectional scanning electron microscopy (SEM) images of TiO_2 thin films with triple-layer structures. The *I-V* curves of dye-sensitized solar cells with triple-layer structures are shown in Figure 8(b). The solar performance parameters of DSSCs with triple-layer structures are listed in Table 5. The efficiencies of DSSCs with the scattering layer prepared by 50, 100, and 200 nm particles are 3.62, 5.68, and 6.54%, respectively. The TiO_2 layers with larger particle sizes on the top layer exhibit higher solar efficiency than that with smaller particle sizes due to the strong back-scattering effect. It is known that smaller particles of TiO_2 layers have large surface area and adsorb more dyes. Hence, it has low contact resistance and high photocurrent. The strong back-scattering light due to large particle size will also increase the reabsorption in the small particle size of TiO_2 layer. This smaller particle size on the bottom is beneficial to recapture the scattering light from the top scattering layer. The larger particle sizes of TiO_2 layers on the top can enhance the back-scattering light effectively and result in higher photocurrent. Thus, the combination of larger particle sizes of TiO_2 on the top and smaller particle sizes of TiO_2 at the bottom will be better for achieving higher solar efficiency.

4. Conclusions

The dye-sensitized solar cells with the TiO_2 prepared by the hydrothermal method have demonstrated good solar performance. A high surface roughness and pure anatase structure are achieved by this method. The dye-sensitized solar cells with the TiO_2 nanorods exhibit higher solar efficiency than that with the commercial TiO_2 particles. The optimal TiO_2 thickness depends on the nanorod sizes of

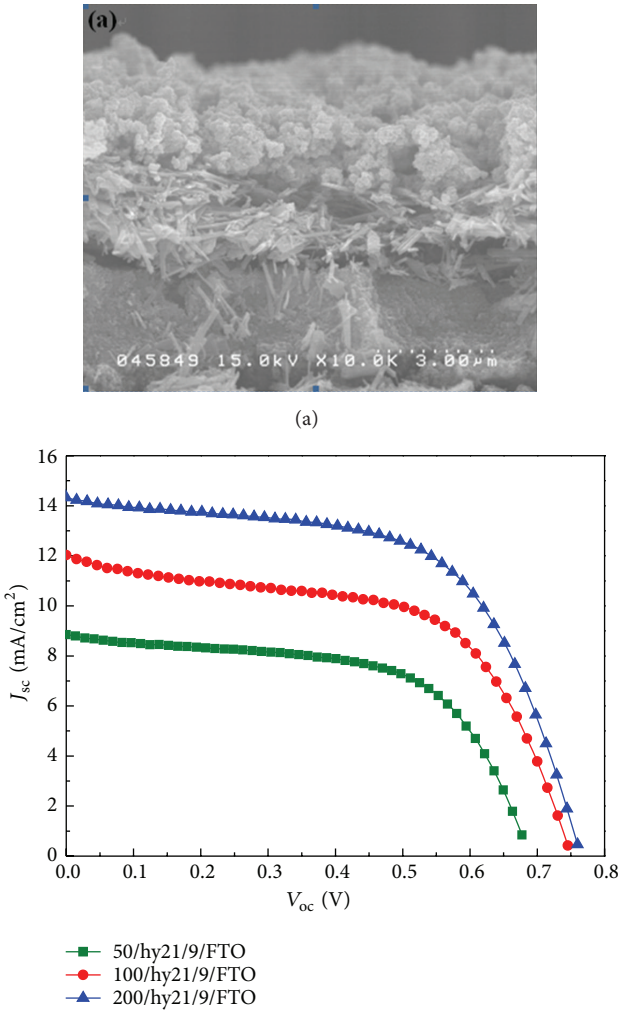

FIGURE 8: (a) The cross-section scanning electron microscopy (SEM) images of TiO_2 thin films with triple layer structures. (b) *I-V* curve of dye-sensitized solar cells with triple layer structures of TiO_2 thin films.

TiO_2 layer for achieving the maximum efficiency. The TiO_2 nanorod size formed through the hydrothermal method will depend on the initial TiO_2 particle size.

Acknowledgment

The authors want to thank the National Science Council of Taiwan, Taiwan, for supporting this research under the Contract no. NSC 100-2221-E-182-037.

References

[1] B. O'Regan and M. Grätzel, "A low-cost, high-efficiency solar cell based on dye-sensitized colloidal TiO_2 films," *Nature*, vol. 353, no. 6346, pp. 737–740, 1991.

[2] M. Grätzel, "Conversion of sunlight to electric power by nanocrystalline dye-sensitized solar cells," *Journal of Photochemistry and Photobiology A*, vol. 164, no. 1-3, pp. 3–14, 2004.

[3] Q. Zhang, C. S. Dandeneau, X. Zhou, and C. Cao, "ZnO nanostructures for dye-sensitized solar cells," *Advanced Materials*, vol. 21, no. 41, pp. 4087–4108, 2009.

[4] S. Ito, T. N. Murakami, P. Comte et al., "Fabrication of thin film dye sensitized solar cells with solar to electric power conversion efficiency over 10%," *Thin Solid Films*, vol. 516, no. 14, pp. 4613–4619, 2008.

[5] D. Kuang, S. Ito, B. Wenger et al., "High molar extinction coefficient heteroleptic ruthenium complexes for thin film dye-sensitized solar cells," *Journal of the American Chemical Society*, vol. 128, no. 12, pp. 4146–4154, 2006.

[6] A. Yella, H.-W. Lee, H. N. Tsao et al., "Porphyrin-sensitized solar cells with cobalt (II/III)-based redox electrolyte exceed 12 percent efficiency," *Science*, vol. 334, no. 6056, pp. 629–634, 2011.

[7] Q. Zhang and G. Cao, "Nanostructured photoelectrodes for dye-sensitized solar cells," *Nano Today*, vol. 6, no. 1, pp. 91–109, 2011.

[8] M. Wei, Y. Konishi, H. Zhou, M. Yanagida, H. Sugihara, and H. Arakawa, "Highly efficient dye-sensitized solar cells composed of mesoporous titanium dioxide," *Journal of Materials Chemistry*, vol. 16, no. 13, pp. 1287–1293, 2006.

[9] W.-G. Yang, F.-R. Wan, Q.-W. Chen, J.-J. Li, and D.-S. Xu, "Controlling synthesis of well-crystallized mesoporous TiO_2 microspheres with ultrahigh surface area for high-performance dye-sensitized solar cells," *Journal of Materials Chemistry*, vol. 20, no. 14, pp. 2870–2876, 2010.

[10] D. Chen, F. Huang, Y.-B. Cheng, and R. A. Caruso, "Mesoporous anatase TiO_2 beads with high surface areas and controllable pore sizes: a superior candidate for high-performance dye-sensitized solar cells," *Advanced Materials*, vol. 21, no. 21, pp. 2206–2210, 2009.

[11] Y. J. Kim, M. H. Lee, H. J. Kim et al., "Formation of highly efficient dye-sensitized solar cells by hierarchical pore generation with nanoporous TiO_2 spheres," *Advanced Materials*, vol. 21, no. 36, pp. 3618–3673, 2009.

[12] F. Sauvage, D. Chen, P. Comte et al., "Dye-sensitized solar cells employing a single film of mesoporous TiO_2 beads achieve power conversion efficiencies over 10%," *ACS Nano*, vol. 4, no. 8, pp. 4420–4425, 2010.

[13] A. C. Zaman, C. B. Üstündağ, F. Kaya, and C. Kaya, "Synthesis and electrophoretic deposition of hydrothermally synthesized multilayer TiO_2 nanotubes on conductive filters," *Materials Letters*, vol. 66, no. 1, pp. 179–181, 2012.

[14] S. K. S. Patel, N. S. Gajbhiye, and S. K. Date, "Ferromagnetism of Mn-doped TiO_2 nanorods synthesized by hydrothermal method," *Journal of Alloys and Compounds*, vol. 509, no. 1, pp. S427–S430, 2011.

[15] J. S. Chen and X. W. Lou, "Anatase TiO_2 nanosheet: an ideal host structure for fast and efficient lithium insertion/extraction," *Electrochemistry Communications*, vol. 11, no. 12, pp. 2332–2335, 2009.

[16] R. H. Lochner and J. E. Matar, *Design for Quality: An Introduction to the Best of Taguchi and Western Methods of Statistical Experimental Design*, Chapman and Hall, New York, NY, USA, 1990.

[17] P. Sharma, A. Verma, R. K. Sidhu, and O. P. Pandey, "Process parameter selection for strontium ferrite sintered magnets using Taguchi L9 orthogonal design," *Journal of Materials Processing Technology*, vol. 168, no. 1, pp. 147–151, 2005.

[18] G. P. Syrcos, "Die casting process optimization using Taguchi methods," *Journal of Materials Processing Technology*, vol. 135, no. 1, pp. 68–74, 2003.

[19] S. S. Mehdi, M. T. Khorasani, and A. Jamshidi, "Hydrothermal processing of hydroxyapatite nanoparticles—a Taguchi experimental design approach," *Journal of Crystal Growth*, vol. 361, pp. 73–84, 2012.

[20] M. Dargahi, H. Kazemian, M. Soltanieh, M. Hosseinpour, and S. Rohani, "High temperature synthesis of SAPO-34: applying an L9 Taguchi orthogonal design to investigate the effects of experimental parameters," *Powder Technology*, vol. 217, pp. 223–230, 2012.

[21] H. P. Wu, C. M. Lan, J. Y. Hu et al., "Hybrid titania photoanodes with a nanostructured multi-layer configuration for highly efficient dye-sensitized solar cells," *The Journal of Physical Chemistry Letters*, vol. 4, no. 9, pp. 1570–1577, 2013.

[22] J.-Y. Liao, B.-X. Lei, D.-B. Kuang, and C.-Y. Su, "Tri-functional hierarchical TiO_2 spheres consisting of anatase nanorods and nanoparticles for high efficiency dye-sensitized solar cells," *Energy and Environmental Science*, vol. 4, no. 10, pp. 4079–4085, 2011.

[23] Z.-S. Wang, H. Kawauchi, T. Kashima, and H. Arakawa, "Significant influence of TiO_2 photoelectrode morphology on the energy conversion efficiency of N719 dye-sensitized solar cell," *Coordination Chemistry Reviews*, vol. 248, no. 13-14, pp. 1381–1389, 2004.

[24] K. Yan, Y. Qiu, W. Chen, M. Zhang, and S. Yang, "A double layered photoanode made of highly crystalline TiO_2 nanooctahedra and agglutinated mesoporous TiO_2 microspheres for high efficiency dye sensitized solar cells," *Energy and Environmental Science*, vol. 4, no. 6, pp. 2168–2176, 2011.

[25] I. G. Yu, Y. J. Kim, H. J. Kim, C. Lee, and W. I. Lee, "Size-dependent light-scattering effects of nanoporous TiO_2 spheres in dye-sensitized solar cells," *Journal of Materials Chemistry*, vol. 21, no. 2, pp. 532–538, 2011.

[26] Y.-C. Park, Y.-J. Chang, B.-G. Kum et al., "Size-tunable mesoporous spherical TiO_2 as a scattering overlayer in high-performance dye-sensitized solar cells," *Journal of Materials Chemistry*, vol. 21, no. 26, pp. 9582–9586, 2011.

[27] M.-J. Jeng, Y.-L. Wung, L.-B. Chang, and L. Chow, "Particle size effects of TiO_2 layers on the solar efficiency of dye-sensitized solar cells," *International Journal of Photoenergy*, vol. 2013, Article ID 563897, 9 pages, 2013.

[28] N.-G. Park, J. Van De Lagemaat, and A. J. Frank, "Comparison of dye-sensitized rutile- and anatase-based TiO_2 solar cells," *Journal of Physical Chemistry B*, vol. 104, no. 38, pp. 8989–8994, 2000.

[29] C. S. Karthikeyan, M. Thelakkat, and M. Willert-Porada, "Different mesoporous titania films for solid-state dye sensitised solar cells," *Thin Solid Films*, vol. 511-512, pp. 187–194, 2006.